Structure and Thermodynamics of Gaseous Oxides, Hydroxides, and Mixed Oxohydroxides of Chromium: $CrO_m(OH)_n$ (m, $n = 0-2$) and CrO_3. A Computational Study

Øystein Espelid,† Knut J. Børve,* and Vidar R. Jensen‡

Department of Chemistry, University of Bergen, Allégaten 41, N-5007 Bergen, Norway

Received: July 16, 1998; In Final Form: October 2, 1998

The geometric structure of nine gaseous molecules obeying the generic formula $CrO_m(OH)_n$ has been determined by gradient-corrected density functional theory, with good agreement with experimental values where available. Cr−ligand bond energies have been determined for all of the molecules by use of the high-level ab initio method CCSD(T) in conjunction with PCI-X and G2(MP2/CC) extrapolation schemes. In combination with computed harmonic vibrational frequencies, the bond dissociation energies are used to form enthalpies of formation. The resulting set represents the best set of consistent values available for the title molecules.

1. Introduction

Thermochemical data are scarce and discrepant for gaseous oxides, hydroxides, and mixed oxohydroxides of many metals. The lack of information is a problem when modeling high-temperature processes, such as hot corrosion of materials. One potential area of application is the construction of solid oxide fuel cells,[1] a development that is severely hampered by obstacles within material design.[2] A particular problem relates to the stability of the material used to couple single fuel cells to stacks.[3] Both alloys and ceramic materials based on chromium are used as interconnector material, and loss of Cr is attributed to chromium oxides and oxohydroxides.[4] The number of chemical species participating in these processes is potentially large, and characterization of the gas-phase composition is difficult. An attractive alternative is to obtain thermodynamical data for the candidate species and then to determine the equilibrium composition of the gas phase under the conditions of the process under study.[5,6] In the following, the present state of knowledge with respect to the enthalpy of formation of the title molecules will be reviewed briefly.

The situation is quite satisfactory for chromium monoxide, for which the two most recent experiments[7,8] agree within 3 kJ/mol for the bond dissociation energy (BDE). The resulting bond strength was confirmed through extensive ab initio calculations by Espelid and Børve in ref 9, henceforth referred to as paper I. These authors also provided what is regarded as accurate enthalpies of formation for gaseous CrOH and CrF. Less is ascertained for the di- and trioxide of chromium, as will be shown in the following for the case of CrO_2. Enthalpies of formation appearing in reference compilations for this molecule are usually based on data published by Grimley et al.[10] in 1961. Whereas the original analysis led to $\Delta_f H° = -58 \pm 60$ kJ/mol, reanalysis by other researchers gave values of -75 ± 40 [11] and -99 ± 5 kJ/mol.[12] On the other hand, a later experiment[13] gave $\Delta_f H° = -13 \pm 30$ kJ/mol, only to be shifted to -46 ± 30 kJ mol when an improved value of $\Delta_f H°(CrO(g))$ became available.[11] A similar disparity exists for $\Delta_f H°(CrO_3(g))$, and the present knowledge of this datum may be indicated by the large error bar stated for the JANAF[11] value, at -293 ± 40 kJ/mol.

Even less information is available for the mixed oxohydroxides of chromium than for the oxides, as discussed in detail in two recent reviews by Ebbinghaus.[12,14] Typically, few and scattered measurements exist for these molecules, and molecular identification is frequently indirect. Lack of molecular structures and vibrational frequencies makes the molecular constant method for estimating temperature effects uncertain. Ebbinghaus resorts to empirical relationships for bond energies between related molecules in order to prepare a complete set of thermodynamical data for these molecules. However, quite large errors must be expected through such procedures, as discussed for Krikorian's fluoride correlation[15] in paper I. The situation is slightly better in the case of chromic acid, for which Glemser and Müller[16] presented vapor data over solid CrO_3, which show good linearity in the concentration and temperature ranges examined.

The purpose of the present contribution is to provide molecular constants and bond energies for a selection of chromium hydroxides, oxides, and mixed oxohydroxides (see Figure 1) by means of quantum chemical calculations. Gradient-corrected density functional theory is used to determine the equilibrium geometry and vibrational frequencies of each molecule. For three of the chromium oxohydroxides, the present work represents the first report on the electronic and geometric structure of the molecule. On the basis of the optimized structures, high-level ab initio quantum chemical methods are used to form accurate bond dissociation energies.

2. Computational Details

DFT calculations and all unrestricted ab initio calculations were performed by means of the Gaussian 94 set of programs.[17] The MolCas package[18] was used for all coupled-cluster calculations based on a restricted closed- or open-shell Hartree−Fock reference state.

2.1. Basis Sets. Most calculations were performed using spherical harmonics bases of valence triple-ζ quality, extended by diffuse functions. Polarization functions were added in two different ways. The simplest set is used for geometry optimizations and includes a single set of polarization functions on hydrogen and oxygen only. This set is denoted by TZD1P. Energy evaluations are based on the TZD2P set, which contains two sets of polarization functions on all elements. Large, segmented bases (SEG-L) are used to compute correction terms for deficiencies in the TZD2P sets, as detailed below. The bases are detailed in paper I.[9] When Dirac−Hartree−Fock calculations

* To whom correspondence should be addressed. E-mail: knut.borve@kj.uib.no.

† E-mail: oystein.espelid@kj.uib.no.

‡ Present address: Max Planck Institut für Kohlenforschung, Kaiser Wilhelm Platz 1, D-45470 Mülheim an der Ruhr, Germany. E-mail: jensen@mpi-muelheim.mpg.de.

10.1021/jp9830427 CCC: $15.00
Published on Web 11/19/1998

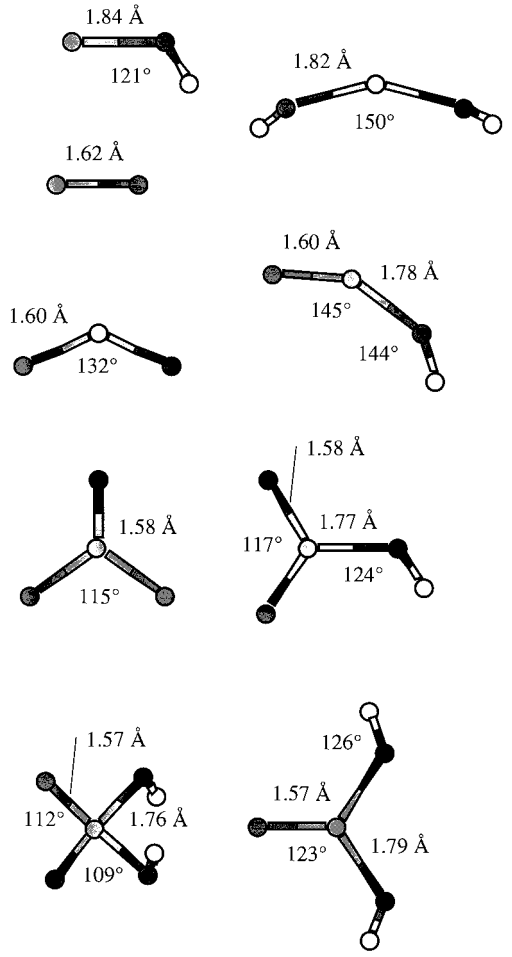

Figure 1. Structures of the molecules discussed in this work, optimized by means of B3LYP/TZD1P.

were performed for CrO_3 and its constituting atoms, the primitive functions making up the TZD2P sets were chosen as bases for the large components, whereas bases for the small components were generated according to the principle of restricted kinetic balance.

2.2. Geometries and Vibrational Frequencies. All geometries were optimized using unrestricted density functional theory (DFT) with TZD1P basis sets as defined above. However, for the closed-shell molecules the resulting wave functions turn out spin-compensated. Exchange was included by means of the Becke three-parameter functional,[19] as implemented in the Gaussian 94[17] sets of programs. This functional includes Hartree−Fock (HF) and Slater exchange as well as Becke's 1988 nonlocal exchange functional correction.[20] Correlation is provided by the functional fitted to the RPA solution of the uniform electron gas by Vosko et al.,[21] conventionally termed VWN3, with local and gradient corrections included in terms of the expression given by Lee et al.[22] The density was evaluated using a grid with 75 radial shells per atom and 302 angular points per shell. Geometries were converged to maximum gradient and displacement of 4.5×10^{-4} au and 1.8×10^{-3} au, respectively. The nature of all stationary points was determined by computing the Hessian analytically. Vibrational frequencies and infrared absorption intensities were obtained within the harmonic approximation. The intensities are referred to as very strong, strong, medium, weak, or very weak, depending on whether the computed intensity is larger than 2.5, in the ranges 0.5−2.5, 0.1−0.5, 0.02−0.1, or below 0.02, in units of $D^2\ u^{-1}\ Å^{-2}$.

2.3. Energy Evaluations. Energy evaluations were performed within the coupled-cluster approximation, including single and double excitation amplitudes (CCSD)[23−25] and with the contributions from connected triples added perturbatively (CCSD(T)).[26] All valence electrons were correlated, and the calculations were carried out in TZD2P atomic bases. The choice of reference states and spin adaptation of the CCSD amplitudes has been given special consideration in a later section.

It is well-known that computed bond energies converge slowly with respect to excitation level and the size of one-particle bases in conventional ab initio treatments. Siegbahn et al.[27−29] proposed the PCI-X scheme to improve this situation, whereby computed correlation effects are scaled by a constant factor to be determined for each computational model. Bauschlicher and Partridge[30] subsequently modified this idea by explicitly computing the main effects from improvement of the one-particle bases by means of second-order Möller−Plesset theory (MP2). Their approach is adopted here, and in addition to the computation of HF, MP2, and CCSD(T) energies in TZD2P bases, restricted HF and MP2 energies are computed also in the SEG-L bases. The resulting combination of medium and large bases coincides well with one example given by Bauschlicher and Partridge,[30] allowing us to adopt their optimized scaling factor of $X = 93.6$ for the computed correlation energy. In summary, basis set corrections relative to TZD2P are obtained as ΔB_{HF} = (RHF/SEG-L − RHF/TZD2P) and ΔB_{MP2} = (RMP2/SEG-L − RMP2/TZD2P), facilitating extrapolated energies as $E_{PCI-X} = E_{HF/TZD2P} + \Delta B_{HF} + (100/X) \times \{E_{CCSD(T)/TZD2P} + \Delta B_{MP2} - E_{HF/TZD2P} - \Delta B_{HF}\}$. For open-shell molecules, unrestricted HF/TZD2P is used in the extrapolation formula to extrapolate dynamic correlation effects only, as discussed in paper I. However, for the closed-shell molecules CrO_3 and $CrO_2(OH)_2$, the unrestricted solution is highly spin-contaminated, and hence, RHF/TZD2P is used in the extrapolation formula. In agreement with paper I, the PCI-X method as applied here is estimated to reproduce bond energies to within 2% of the computed correlation effects. This implies error bars for bond dissociation energies that increase with increasing oxidation state on chromium, since the impact from extrapolation increases. Specifically, error bars of 0.10 and 0.15 eV seem reasonable for Cr−oxo bond strengths in molecules where the formal oxidation number of Cr, Ω, obeys $\Omega < +V$ and $\Omega \geq +V$, respectively. The variation is less for Cr−OH bond energies, and a conservative error estimate of 0.10 eV is applicable throughout the present series of molecules.

Another highly efficient extrapolation procedure is the G2 method by Pople and co-workers,[31] which we will use in a modification denoted by G2(B3LYP/MP2/CC).[32] Here, electronic energies are obtained as $E_{G2} = E_{CCSD(T)/TZD2P} + \Delta B_{MP2} - An_\alpha - Bn_\beta$, where n_α (n_β) is the number of valence electrons with α (β) spin ($n_\alpha \geq n_\beta$, by convention) and A and B are semiempirical constants. In contrast to PCI-X, extrapolation to complete bases and high excitation orders is performed by additive correction terms. When a molecule XY homolytically dissociates into fragments X and Y, this correction will, in most cases, increase the computed dissociation energy by an amount k(B−A), where k is the formal number of electron pairs participating in the bond. Using the latest experimental value of D_0(CrO) for calibration leads to B−A = 11.6 kJ/mol, which is close to 11.3 kJ/mol computed from the A and B values quoted in ref 32. However, in Table 1 in ref 30 Bauschlicher and Partridge use B−A = 2.1 kcal/mol (=8.8 kJ/mol) with one-particle bases similar to ours. This value is determined in a fit

to experimental atomization energies for 55 first- and second-row molecules. Here, we use an average value of B−A = 10.1 kJ/mol and adopt error bars sufficiently wide to encompass any energetic effect of reoptimizing the additive correction. On the basis of mean absolute errors in bond energies for the calibration set in ref 32, error bars of $\Omega \times 6$ kJ/mol are accepted for the computed enthalpies of formation, where Ω is the formal oxidation number of the chromium species in consideration.

The contribution from correlating electrons in the outer core of chromium, e.g., 3s and 3p, was found in paper I to be small for CrO and CrOH. In this work, core-correlation was examined in the case of chromium dioxide by means of the CCSD(T) method in conjunction with SEG-L bases. Whereas the core-correlation contribution toward atomization was computed to −0.10 eV, basis-set superposition constitutes half this number, as estimated by the counterpoise method. Thus, considering the size of the contribution, its susceptibility to BSSE, and the computational cost, it was decided to omit core-correlation terms throughout this study.

All computed energies were converted to enthalpies at 298 K by treating translation and rotation classically, by subtracting contributions from *PV* work as for ideal gases, and by computing the vibrational energy according to equations for the harmonic oscillator. Zero-point vibrational energies (ZPVEs) have been shown to be accurately reproduced by the B3LYP method.[32,33] Scaling factors of 0.98[32,33] and 0.99,[32] depending on the choice of basis sets, are proposed for improving the computed ZPVEs further. Scaling would, if applied to the fragmentation of chromic acid to separate metal atom and ligands, amount to a reduction of less than 0.01 eV in the contribution from ZPE to the total binding energy, which is some 17 eV at the B3LYP/TZD2P level of accuracy. Hence, no scaling of the ZPVEs has been performed.

3. Results and Discussion

3.1. Homing the Computational Methodology. As will be demonstrated, the present set of molecules exemplify highly complex electronic structures. Numerous tests have been carried out to ensure that the computational methods applied here are well adapted to face these problems. The present section is to make the experience from this process available to other workers in the field.

3.1.1. Selection of an Appropriate DFT Method. Density functional methods have been shown to provide reliable geometries and vibrational frequencies for compounds containing transition metal atoms.[34] However, a range of different functionals are reportedly used to this end, with different merits depending on the precise kind of systems. To aid our choice of functionals, the ability to reproduce electron affinities of oxygen and hydroxyl as well as bond energies of chromium monoxide and chromium hydroxide has been examined for six different combinations of exchange and correlation functionals, referred to by their Gaussian-94 acronyms (see Table 1). The Perdew 1986 (P86) correlation functional[35] systematically leads to exaggerated estimates of the electron affinities and is disqualified for this reason. All examined DFT methods reproduce the bond strength in CrOH within 0.2 eV of the value recommended in paper I, with particular high accuracy for the functionals denoted by BPW91, B3LYP, and B3P86. On the other hand, only B3LYP and B3P86 manage a similar accuracy for the strength of the double bond in the monoxide. Hence, among the gradient-corrected functionals considered here, the HF-DFT hybrid B3LYP appears superior, slightly underestimating the recommended values of D_0(Cr−O) and D_0(Cr−OH) by 0.09 and 0.05 eV, respectively, while providing good estimates of the electron affinities of the relevant ligands. On the other hand, BPW91 may provide competitive estimates of the bond strengths between chromium and hydroxyl and will be used in this study to exemplify the potentials of a pure DFT method.

TABLE 1: Comparison of Various DFT Methods with Respect to Electron Affinities of O and OH and Bond Strengths in CrO and CrOH (All Quantities in eV)

	EA(O)	EA(OH)	D_0(CrO)[a]	D_0(Cr−OH)[a]
BLYP	1.81	1.94	5.51	3.93
BP86	1.90	2.06	5.51	3.93
BPW91	1.70	1.89	5.22	3.75
B3LYP	1.67	1.83	4.60	3.69
B3P86	2.12	2.31	4.63	3.72
B3PW91	1.50	1.71	4.35	3.53
literature	1.461[b]	1.828[b]	4.74,[c] 4.69[d]	3.86,[e] 3.74[d]

[a] Includes relativistic correction taken from paper I. [b] Lide, D. R., Ed. *CRC Handbook of Chemistry and Physics*, 76th ed.; CRC Press: Boca Raton, FL, 1995. [c] Reference 8. [d] Paper I. [e] Gorokhov, L. N.; Milushin, M. I.; Emelyanov, A. M. *High Temp. Sci.* **1990**, *26*, 395.

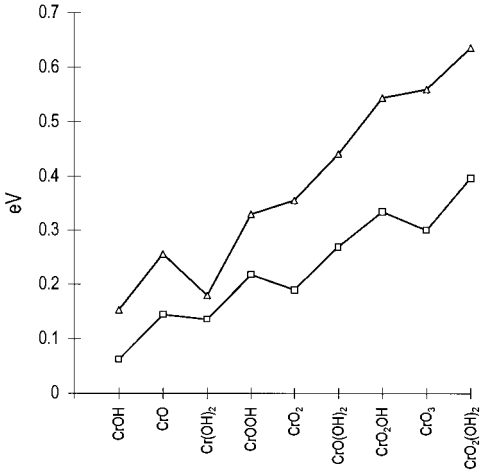

Figure 2. Contribution from relativistic effects toward the atomization energy of selected molecules, as estimated by first-order perturbation theory based on RHF wave functions (1PT/RHF; △) and quasi-relativistic DFT theory (QR/BP86; □).

3.1.2. Contribution from Relativity to Chromium−Ligand Bond Strengths. Even though chromium is a first-row transition metal, one must expect important contributions from relativistic effects to metal−ligand bond strengths in some of the molecules studied here. In paper I, a relativistic contribution of 0.26 eV to D_0(CrO) was obtained, and this contribution is likely to increase as the oxidation state of chromium increases through the series of title molecules. This expectation is born out in Figure 2, where two different methods have been used for estimating the scalar relativistic contributions to energies of atomization. However, even though both methods agree upon the trend, they differ significantly when it comes to absolute numbers. First-order perturbation theory, including mass−velocity and Darwin terms and applied to RHF wave functions (1PT/RHF), is seen to give persistently larger relativistic corrections than does the quasi-relativistic DFT-based approach (QR/DFT). This is surprising in that earlier studies report that the 1PT and QR approaches are equally adequate for valence levels of elements up to $Z = 70$.[36] In order to choose between these two methods of obtaining relativistic corrections, chromium trioxide was used as the test system. The discrepancy between 1PT/RHF and QR/DFT is particularly large for this molecule, cf. values of 0.56 vs 0.30 eV for the atomization

process, and the closed-shell structure of CrO_3 makes it amenable to more accurate procedures, to be discussed below.

The quasi-relativistic correction is computed from orbitals optimized for the BP86 density functional, which contains both local and nonlocal electron correlation terms, whereas 1PT/RHF estimates are based on uncorrelated wave functions. Thus, a first guess as to the cause for disparate values may be notable coupling between relativity and electron correlation. However, the quasi-relativistic estimate is essentially unchanged when computed from orbitals obtained in the Hartree−Fock−Slater (Xα) approximation. Correspondingly, the 1PT correction for atomization of CrO_3 decreases by merely 0.03 eV when computed from a valence-correlated MCPF[37] wave function. Hence, it appears that one is justified in treating the relativistic effect separately from correlation effects.

To get accurate numbers for the relativistic contribution to the atomization energy of chromium trioxide, it was decided to perform all-electron Dirac−Hartree−Fock (DHF) calculations for this system by means of the DIRAC program.[38] DHF calculations for atomic oxygen and chromium were performed by means of GRASP,[39] which, however, imposes spherical symmetry and only allows orbitals to be optimized for an average of states having the specified total angular momentum and electron configuration. These restrictions were subsequently relaxed in separate RHF calculations for the atoms, and the final relativistic correction to the atomization energy of CrO_3(g) was determined to 0.555 eV. The agreement with 1PT/RHF is excellent, whereas the QR/DFT value of 0.30 eV is decisively too low. Hence, 1PT/RHF is the favored scheme for obtaining relativistic corrections, to be included in all reported bond energies and enthalpies.

Some attempts were made to analyze the failure of the DFT-based quasi-relativistic approach. First, the formal improvements in the QR approach, relative to 1PT, were shown to be unimportant for these light atoms in that 1PT/DFT gave results in good agreement with QR/DFT results. Next, differences with regard to relaxation of core orbitals were shown to be of little consequence. At this point, we do not understand the discrepancy evident in Figure 2.

3.1.3. Selection of an Appropriate ab Initio Correlation Method. The coupled cluster (CC) method is recognized as a powerful technique in computational quantum chemistry. In particular, at the level of truncated singles and doubles excitation (CCSD) plus perturbative estimate of the contribution from connected triple excitations, i.e., CCSD(T),[40] it is generally regarded as an accurate and robust method for computing both energy differences and properties of molecules. The choice of orbitals to be used in the reference state has been discussed by various authors. Considerations that come into play concern spin contamination, orbital instability toward symmetry breaking, and formal inclusion of fifth-order terms in many-body perturbation theory. The CCSD wave function is shown to be insensitive to the choice of UHF or RHF reference state in the presence of mild spin contamination.[41] However, the choice of Brueckner orbitals, which eliminates the amplitudes of single excitations, proves superior as spin contamination gets more serious.[42] The resulting "Brueckner doubles" (BD) expansion is also recommended when symmetry breaking occurs at the SCF level of accuracy.[43] Even though inclusion of the triples estimate (T) significantly improves the accuracy of both CCSD and BD, it also leads to increased susceptibility toward orbital instability.[44]

The molecules discussed in this paper contain weak π bonds between chromium and terminal oxygen atoms. A proper description of these bonds relies heavily on the ability to correlate both σ and π electrons and to some extent also lone pairs at the ligand. Failure to do so leads to excessive spin contamination, arising from the localization of α and β spin orbitals, to chromium and the terminal oxygen atoms. An additional problem arises in those of the molecules that possess a delocalized π system, in that the Hartree−Fock orbitals will, if given the flexibility, localize the π bond and hence break the symmetry present in the nuclear framework. These problems are almost absent in the single-determinant B3LYP description, since the orbitals are determined in a correlated self-consistent field. For this reason, the identification of ground-state electronic states and equilibrium structures is carried out at the DFT level of accuracy. However, accurate energy differences require the use of high-level ab initio theory, and detection of the present difficulties warrants a judicious choice of methodology.

TABLE 2: Bond Dissociation Energies As Computed in Various CCSD(T) Formalisms[c]

ref state	cluster expansion	D_0(CrX−Y) (eV)			
		Cr−O	CrO−O	CrO_2−O	Cr−OH
UHF	UCCSD(T)[a]	4.15	4.94	4.39	3.58
RHF	UCCSD(T)[a]	4.28	5.00	4.22	3.56
RHF	RCCSD(T)[b]	4.18	5.04	4.29	3.54
UHF	UBD(T)[a]	4.16	5.08	4.35	3.58

[a] No spin adaptation. [b] The CCSD calculations are spin adapted according to T2 DDVV [Neogrády, P.; Urban, M.; Hubac, I. *J. Chem. Phys.* **1992**, *100*, 3706], whereas the triples estimate is obtained in a strictly restricted formalism. [c] All energies include relativistic corrections.

In Table 2, bond dissociation energies are reported for the chromium oxides and chromium hydroxide, as computed using various reference states and spin adaptation schemes in the CCSD(T) and BD(T) expansions. D_0(Cr−OH) is almost invariant between the methods, thus reflecting the robustness of the CCSD expansion as usually found. However, rather large differences are obtained for the oxides, even for the monoxide, which does not suffer from symmetry breaking in the usual sense. The effect of changing from the UHF to RHF reference state is 0.13 eV, which agrees well with the difference of 0.12 eV reported by Bauschlicher and Maitre.[45] They claim the RHF-based calculation to be the better, since it results in a higher bond strength. However, we find that if the CC expansion is spin-adapted to avoid contamination of the CCSD wave function, the resulting energy agrees much more closely with the UHF/UCCSD(T) result than with the RHF/UCCSD(T) result. Furthermore, this energy is corroborated by Brueckner doubles calculations. As pointed out previously, BD is generally perceived to be insensitive to the choice of restricted or unrestricted reference determinant. This was confirmed in the present study for the molecule showing the highest degree of spin contamination, CrO_3. Even though the UCCSD(T) estimate of $D_0(CrO_2-O)$ experiences a substantial shift of +0.17 eV when changing from the restricted to the unrestricted reference state, cf. Table 2, the corresponding shift for UBD(T) is down to +0.03 eV when computing the energy of CrO_3 with a restricted reference state (not included in the table). Generally, the best agreement between CCSD(T) energies and UBD(T) energies is found for the spin-adapted expansion based on a restricted Hartree−Fock reference state. Because of large differences in efficiency between the implementations of UBD-(T) and RCCSD(T), which were available to us, the latter method is chosen for computing bond dissociation energies.

3.2. Characterization of Electronic Ground States. In order to aid the discussion of structure and bonding of the title

TABLE 3: Characterization of Valence Molecular Orbitals Occupied in the Ground States of the Title Molecules

molecule	term[a]	valence orbitals[b]
CrOH	^{6}A′ [C_s]	9a′}w$\underline{\sigma}$ a′}w$\underline{\sigma}$ 3a″}L a′}^{1}d a′}^{1}d,w$\underline{\sigma}$ a″}^{1}d a′}^{1}d a″}$^1\underline{\pi}$*
CrO	$^5\Pi$ [$C_{\infty v}$]	9σ}σ 3π}π σ}^{1}d 1δ}^{2}d π}$^1\pi$*
$Cr(OH)_2$	^{5}B [C_2]	8a}w$\underline{\sigma}$ 7b}L a}w$\underline{\sigma}$ b}$\underline{\sigma}$ a}L b}L a}^{1}d b}^{1}d a}^{1}d a}^{1}d,w$\underline{\pi}$*
CrOOH	^{4}A″ [C_s]	12a′}w$\underline{\sigma}$ a′}σ,$\underline{\pi}$ 3a″}π,$\underline{\pi}$ a′}σ a′}L a″}L a′}^{1}d a″}^{1}d a′}$^1\underline{1}\sigma$*
CrO_2	$^3B_1$ [C_{2v}]	8a$_1$}σ 5b$_2$}σ 1a$_2$}π a$_1$}L,wσ 3b$_1$}L,wπ b$_2$}L a$_1$}^{1}d,wσ* b$_1$}^{1}d,wπ*
$CrO(OH)_2$	^{3}A″ [C_s]	5a″}$\underline{\sigma}$ 12a′}L a′}σ,w$\underline{\sigma}$ a′}π a″}L a′}L a″}L a′}L a″}L a′}^{1}d,wσ* a″}^{1}d,w$\underline{\pi}$*
CrO_2OH	^{2}A′ [C_s]	14a′}w$\underline{\sigma}$ a′}w$\underline{\sigma}$,σ,π a′}σ,π 3a″}π a′}L,w$\underline{\sigma}$,wσ a″}$\underline{\pi}$,π a″}L a′}L a′}L a′}$^1\underline{1}$d
CrO_3	^{1}A$_1$ [C_{3v}]	e}σ,π e}π a$_1$}σ a$_1$}L e}L 1a$_2$}L
$CrO_2(OH)_2$	^{1}A [C_2]	10a}w$\underline{\sigma}$ 9b}w$\underline{\sigma}$ [a b a a b][c] b}L a}L a}L b}L b}L

[a] The point group of the equilibrium ground-state geometry is included in square brackets. [b] The orbitals are listed by their symmetry designation according to increasing orbital energy and further characterized by the following: L (localized to ligands as lone pair or σ_{O-H}), d (Cr 3d, possibly hybridized with 4s), $\sigma(\underline{\sigma})$ Cr−oxo (Cr−hydroxo) σ bonding, $\pi(\underline{\pi})$ Cr−oxo (Cr−hydroxo) π bonding. Antibonding interaction is denoted by an asterisk, whereas weak interactions are flagged by a preceding "w". Occupation numbers are included only for open shells, and the ordinal number is included only for the first valence orbital of a given symmetry for each molecule. [c] Bonding orbitals showing decreasing overlap between metal and ligands with higher energy.

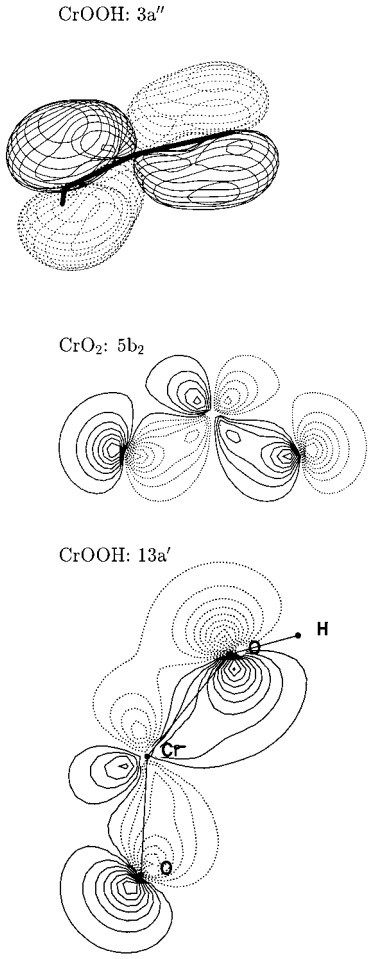

Figure 3. Isosurface of the strongly π-bonding 3a″ orbital in CrOOH (top), contours in the molecular plane of $5b_2$ in CrO_2 (middle), and 13a′ in CrOOH (bottom). See text.

molecules, the occupied valence orbitals are listed in Table 3 for the ground states. The orbitals are tentatively characterized by their properties with respect to bonding between Cr and the ligands, i.e., the molecular orbitals arising from interactions between Cr 3d4s and O 2p atomic orbitals. Bond orders in the sense of Baders atoms-in-molecule theory[46] were computed[47] at the B3LYP/TZD1P level of accuracy, and for all molecules, bond orders close to 1 were found between chromium and hydroxo ligands, as opposed to close to 2 between chromium and oxo ligands. This indicates that the covalent character between chromium and each kind of ligand is comparable throughout the present series of molecules. On the other hand, the net atomic charge on chromium increases only up to the equivalent of a full electron missing, which occurs at an oxidation number of IV. Increasing the oxidation number further leads to lower net atomic charges at the ligands, indicating less pronounced ionic character and lower contribution from electrostatics to bond energies. Taking both covalent and ionic characters into consideration, bond strengths may be expected to reach maximum for molecules with chromium in an intermediate oxidation state (III, IV, and V). For two of the molecules, CrOOH and CrO_2OH, orbitals with pronounced π bonding interaction between chromium and hydroxo ligands are found, as indicated in Table 3 and shown in Figure 3 (top).

TABLE 4: Structure Elements Related to the Oxide Functionality in Selected Chromium Oxides and Oxohydroxides

molecule	$R_{Cr=O}$ (Å)	$A_{O=Cr=O}$ (deg)	$A_{O=Cr-OH}$ (deg)	Θ[a] (deg)
CrO	1.622			
CrOOH	1.602		144.5	0
CrO_2	1.603	132		
$CrO(OH)_2$	1.568		122.5	28
CrO_2OH	1.581	117.1	123, 120	0, −180
CrO_3	1.584	115.1		
$CrO_2(OH)_2$	1.566	111.5	110, 108	212, −26

[a] Dihedral angle O═Cr−O−H.

3.3. Molecular Structures and Vibrational Frequencies. The aim of this section is to present structural parameters and vibrational frequencies, as computed for the molecules under consideration, and to assess the accuracy that may be attributed to these data. An overview of the molecular structures is given in Figure 1.

Bond lengths, bond angles, and torsion angles pertaining to oxo ligands are presented in Table 4, and vibrational harmonic frequencies of modes dominated by these internal coordinates are listed in Table 5. The bond between chromium and terminal oxygens is typically shortened with increasing oxidation number of the metal, and the corresponding stretching frequencies increase by 100 cm^{-1} from chromous acid, CrOOH, to chromic acid, $CrO_2(OH)_2$. This trend may be due to reduced repulsion between metal d electrons and the negatively charged ligands. $CrO(OH)_2$ presents an exception to this pattern by displaying a very short Cr═O bond, almost as short as in chromic acid. The extra bond shortening is probably due to the contribution of a localized π bond. In contrast, the trioxide displays a bond length that is 0.022 Å longer than the one in chromic acid, despite having the same oxidation number, +VI.

TABLE 5: Computed Harmonic Vibrational Frequencies[a] and IR Intensities[b] Related to the Oxide Functionality

molecule	ν(Cr═O) (cm^{-1})	δ(O═Cr═O) (cm^{-1})	δ(O═Cr−OH) (cm^{-1})	τ(O═Cr−O−H) (cm^{-1})
CrO	864 (vs)			
CrO_2	982 (s), B_1 1038 (vs)	224 (s)		
CrO_3	999 (m)	209 (s)		
	E 1073 (vs)	E 372 (vw)		
CrOOH	985 (vs)		147 (m)	A″ 422 (vs)
$CrO(OH)_2$	1060 (vs)		A″ 223 (m)	124 (s), A″ 128 (s), 270 (vs)
CrO_2OH	1041 (s) 1058 (vs)	340 (w)	233 (m)	A″ 18 (s), A″ 534 (vs)
$CrO_2(OH)_2$	1081 (s), B 1110 (vs)	401 (s)	B 295 (m), B 324 (vw)	221 (s), 341 (s), B 363 (s)

[a] The symmetry of the mode is included if different from the fully symmetric irreducible representation. [b] IR absorption intensities are characterized by v (very), s (strong), m (medium), and w (weak) as outlined in Computational Details.

TABLE 6: Structure Elements Related to the Hydroxo Ligand

molecule	R_{Cr-OH} (Å)	R_{O-H} (Å)	A_{Cr-O-H} (deg)	$A_{HO-Cr-OH}$ (deg)
CrOH[a]	1.838	0.964	121	
$Cr(OH)_2$	1.819	0.962	130	150[b]
CrOOH	1.783	0.960	144	
$CrO(OH)_2$	1.788	0.963	126	114
CrO_2OH	1.766	0.967	124	
$CrO_2(OH)_2$	1.764	0.969	115	110

[a] Paper I. [b] The dihedral angles τ(OCrOH) in $Cr(OH)_2$ are 287°.

The OCrO bond angle is markedly less pointed in the dioxide than in the molecules with three or more ligands, and the computed value of 132° agrees well with the most recent experimental result of 128° ± 4°.[48] Similarly, the O−Cr−OH angle is much wider in CrOOH than in the larger molecules. Within the VSEPR model these molecules are expected to have a linear arrangement about chromium, since unshared d electrons are usually regarded as stereochemically inactive. However, in the linear geometry, the only σ bond that chromium is able to form to its ligands is of two-electron-three-center character, since the valence orbitals of chromium are of even parity. Upon bending, one of the $3d_\pi$ components facilitates elements of σ bonding, cf. Figure 3 (middle), and this is probably the driving force of departure from linearity. According to B3LYP calculations, in chromium dioxide the linear structure lies 37 kJ/mol higher in energy than the equilibrium geometry. Furthermore, the bonds are stretched by 0.03 Å, consistent with a reduction in σ bonding. It is interesting to note that in CrOOH, the CrOH angle is exceptionally wide compared to the other molecules (cf. Table 6). This demonstrates the dual role of the in-plane Cr $3d_\pi$ component, which retains some π-bond character toward the hydroxo ligand, as shown in Figure 3 (bottom). In addition to the perpendicular π-bonding components already mentioned for CrOOH and CrO_2OH, this is the only notable example of other than single-lobe overlaps between Cr 3d and oxygen 2p found for the hydroxo ligands in the present series of molecules.

CrO_3 is found to be slightly nonplanar, with chromium some 0.36 Å above a plane defined by the oxygen atoms. The energy lowering compared to a D_{3h} structure is only on the order of 4 kJ/mol, however. The departure from planarity facilitates 4p3d hybridization along the axis of rotation, but the Cr 4p population remains very low, and the reason for the out-of-plane torsion is not well understood.

Within the present model chemistry, bond lengths of 0.978 and 0.969 Å are obtained for the hydroxyl radical and hydroxide anion, respectively. The latter value is close to or slightly larger than what is computed for chromium monohydroxide and the oxohydroxides (see Table 6). A trend toward longer and softer OH bonds with increasing charge on chromium is discernible in Tables 6 and 7, but the effects are minor. On the other hand, the Cr−OH bond lengths seem to be stepped down by the number of oxo moieties in the molecule. This may be understood in terms of a steady decrease in bond length with increasing oxidation state of chromium, modulated by extra bond shortening in CrOOH and CrO_2OH because of the presence of π bonding as noted above.

In the mixed oxohydroxides, structures where hydrogen is pointed toward terminal oxygen atoms are consistently found to be favored energetically. However, the distance between a hydrogen atom and the closest oxo moiety is too long for intramolecular hydrogen bonding, and it is seemingly determined by how crowded the molecule is rather than the strength of the OH−O interaction; that is, the distance decreases from 3.88 Å in CrOOH to 2.82 Å in chromic acid, with intermediate numbers of 3.20 and 3.28 Å for the mixed complexes with three ligands.

Of the present molecules, the metal−ligand bond length has been determined experimentally[49] only for the diatomic CrO(g), giving a value of 1.618 Å, i.e., only 0.004 Å shorter than that computed in this work. To facilitate further comparison, the present computational model has been applied to CrF(g) and CrO_2F_2(g), which are isoelectronic to CrOH and $CrO_2(OH)_2$, respectively. For the diatomic, the computed bond length is 0.024 Å too long, as discussed in paper I.[9] In the closed-shell chromyl fluoride, measured[50] and computed structural parameters are as follows. Bond length (Å) R(Cr−F): exptl, 1.716(2); calcd, 1.721. R(Cr═O): exptl, 1.572(2); calcd, 1.556. Bond angle (deg) A(OCrO): exptl, 107.8(8); calcd, 108.3. A(FCrF):

TABLE 7: Computed Harmonic Vibrational Frequencies[a] and IR Intensities[b] Related to the Hydroxo Ligand

molecule	ν(O−H) (cm^{-1})	ν(Cr−OH) (cm^{-1})	δ(Cr−O−H) (cm^{-1})	δ(HO−Cr−OH) (cm^{-1})
CrOH	3833 (s)	628 (s)	608 (vs)	
$Cr(OH)_2$	B 3862 (vs), 3863 (m)	B 726 (vs), 621(s)	B 489 (vs), 571(m)	82 (w)[c]
CrOOH	3905 (vs)	714 (s)	506 (vs)	
$CrO(OH)_2$	3857 (s), A″ 3853 (vs)	682 (m), A″ 752(vs)	A″ 567 (vs), 622 (vs)	205 (m)
CrO_2OH	3820 (vs)	741 (s)	588 (vs)	
$CrO_2(OH)_2$	3794 (s), B 3789 (vs)	730 (s), B 746 (vs)	792 (s), B 796 (w)	268 (s)

[a] The symmetry of the mode is listed only if different from the fully symmetric irreducible representation. [b] IR absorption intensities are characterized by v (very), s (strong), m (medium), and w (weak) as outlined in the Computational Details section. [c] $Cr(OH)_2$ also possesses symmetric and antisymmetric τ(HO−Cr−OH) twisting modes at 299 (s) and B 402 (vs) cm^{-1}, respectively.

TABLE 8: PCI-X and G2(MP2/CC) Estimates of Chromium−Oxo Bond Strengths, Resolved into Various Contributions (All Quantities in eV)

bonds CrX−O	relativity[a] + ZPVE[b]	ΔB_{MP2}[c]	HF[d] + ΔB_{HF}[c]	RCCSD(T)	D_0(CrX−O) G2(MP2/CC)[e]	D_0(CrX−O) PCI-X[f]
Cr−O	0.20	0.32	0.34	3.98	4.71	4.77
CrOH−O	0.08	0.30	0.42	5.06	5.65	5.77
CrO−O	0.01	0.24	−0.13	5.03	5.49	5.65
$Cr(OH)_2$−O	0.17	0.27	−0.78	4.62	5.28	5.46
CrO(OH)−O	0.11	0.21	−2.32	4.48	5.01	5.28
CrO_2−O	0.09	0.24	−3.17	4.20	4.75	5.06
$CrO(OH)_2$−O	0.03	0.12	−3.62	4.13	4.49	4.81

[a] Computed according to 1PT/RHF. [b] Zero-point vibrational energy. [c] Basis-set correction computed as outlined in Computational Details. [d] UHF (RHF) for open (closed) shell molecules. [e] Includes an additive correction amounting to 0.21 eV for D_0(CrX−O). [f] PCI-X extrapolated estimate, with $X = 93.6$ and basis set correction according to ref 30.

exptl, 111.9(9); calcd, 110.2. *A*(OCrF): exptl, 109.3(2); calcd, 109.6. For the experimental values, the uncertainty in the last decimal is indicated in parentheses. Generally, the agreement is very good between the two structures. The largest error occurs for the oxo bonds, which are computed 0.016 Å too short. The fluoride bond lengths are essentially correct, whereas the largest error in bond angles is found for the F−Cr−F angle, which is computed to be slightly narrow. In paper I it was shown that the bond length in the hydroxide anion is reproduced by the present methodology, whereas the prediction for the neutral hydroxyl radical is too high by 0.007 Å. The bond length computed for chromium trioxide is essentially identical to what was obtained by Ziegler and Li[51] in the local spin density approximation (LSDA). Furthermore, their reported structural parameters for CrO_2OH fit well with those listed in Tables 4 and 6. Some differences exist in the OH bond length and Cr−O−H bond angle, however. These are caused in equal amounts by neglect of gradient corrections in the density functional used for geometry optimization and the less flexible oxygen basis used in ref 51.

Observed vibrational frequencies of the chromium oxides are available for comparison. Whereas the frequency obtained in paper I for CrO was slightly low compared to the experimental value of 898.5 cm^{-1},[49] the opposite is found to be the case when the molecule possesses a delocalized π bond between chromium and oxygen. In chromium dioxide the observed frequencies are 914.4 cm^{-1} (ν_1),[48] 965.4 cm^{-1} (ν_3),[48] and 220 ± 20 cm^{-1} (ν_2),[52] corresponding to computed values of 982 and 1038 cm^{-1} for the symmetric and antisymmetric stretching modes, respectively, and 224 cm^{-1} for the bending mode. CrO_3(g) is reported[53] to absorb at 995 cm^{-1} in the infrared region, which may be compared to a computed frequency of 1073 cm^{-1} for the doubly degenerate stretching mode in this molecule. The symmetric A_1 mode is also IR active, and even though the computed frequency of 999 cm^{-1} fits nicely with the experimental value, the low intensity makes it a less likely candidate for detection. Our computed frequency for the bending mode of E symmetry, 372 cm^{-1}, is close to the observed frequency of 350 cm^{-1}. Thus, in both of the higher oxides, the calculations overestimate the frequencies of the Cr═O stretching modes by some 70−80 cm^{-1}. As for the structural parameters, it is interesting to see how well the present methodology describes the vibrations in chromyl fluoride, CrO_2F_2(g). A complete set of fundamental frequencies have been published for this molecule,[54] and they may be compared to our computed values as follows, in units of cm^{-1}. A_1 δ(F−Cr−F): exptl, 208; calcd, 216. A_2 τ(F−Cr−F): exptl, 259; calcd, 282. B_1 δ(F−Cr−F): exptl, 274; calcd, 296. B_2 δ(F−Cr−F): exptl, 304; calcd, 321. A_1 δ(O═Cr═O): exptl, 364; calcd, 420. A_1 ν(Cr−F): exptl, 727; calcd, 731. B_2 ν(Cr−F): exptl, 789; calcd, 778. A_1 ν(Cr═O): exptl, 1006; calcd, 1105. B_1 ν(Cr═O): exptl, 1016; calcd, 1113. Here, the axis system is chosen such that B_1 changes sign under reflection in the plane spanned by CrF_2. Generally, the agreement between theory and experiment is very satisfactory, in particular for the frequencies pertaining to the chromium−fluoride bonds. However, as found above in the case of the di- and trioxides, stretching frequencies of the oxo bonds are overestimated, here by 100 cm^{-1}. Even though it is conceivable that anharmonic effects are important for these molecules, the previously noted underestimation of oxo bond lengths, by 0.016 Å in chromyl fluoride, suggests that the explanation for the overestimated frequencies lies elsewhere. Indeed, since molecular parameters pertaining to both chromium monoxide and the Cr−F bonds in CrO_2F_2 are very well reproduced by theory, it is likely that the problem lies in the DFT description of the delocalized π component when chromium is bonded to more than one oxo ligand. Still, the accuracy achieved both for vibrational frequencies and for structural parameters is highly satisfactory, and most importantly, will not present a limiting factor for the computed bond strength. Assuming a generous force constant of 15 mdyne/Å for a chromium−oxygen double bond, a compression of the bond by 0.02 Å represents an energy of only 0.01 eV.

3.4. Bond Energies and Enthalpies of Formation. The main purpose of the present work is to compute reliable metal−ligand bond strengths for the molecules under consideration, a task that presupposes the use of high-level ab initio methods in conjunction with some kind of extrapolation scheme. The methodologies favored here are based on RCCSD(T) energies, extended by basis-set corrections computed by means of RMP2, and extrapolated according to the PCI-X and G2(MP2/CC) schemes. Resulting Cr−oxo and Cr−hydroxo bond dissociation energies (BDE's) are given in Tables 8 and 9, respectively, along with quantities needed for their construction from the formulas given under Computational Details.

3.4.1. Bond Dissociation Energies. In Figure 4, chromium−oxo bond energies, as computed using DFT and ab initio methods, are plotted in order of increasing oxidation state of the metal. Also included are bond energies as estimated by Ebbinghaus[14] on the basis of experimental data and empirical correlations. The same trend in BDE is conveyed by all theoretical methods: an initial increase to a maximum bond strength for chromous acid, CrOOH, followed by a slow decline. This kind of behavior was anticipated from the population analysis, based on almost constant bond orders and saturation of the net charge of chromium. Contrary to this, the Cr−oxo bonds become gradually shorter, probably because of reduced repulsion of Cr 4s3d electrons. When the various computational models are compared, the DFT methods are seen to bracket the two extrapolated ab initio curves, PCI-X and G2(MP2/CC), with

TABLE 9: PCI-X and G2(MP2/CC) Estimates of Chromium−Hydroxo Bond Strengths, Resolved into Various Contributions (All Quantities in eV)

bonds CrX−OH	relativity[a] + ZPVE[b]	ΔB_{MP2}[c]	HF[d] + ΔB_{HF}[c]	RCCSD(T)	D_0(CrX−OH) G2(MP2/CC)[e]	D_0(CrX−OH) PCI-X[f]
Cr−OH	0.07	0.14	2.19	3.47	3.79	3.78
Cr(OH)−OH	0.11	0.17	2.46	4.10	4.26	4.28
CrO−OH	−0.06	0.13	2.27	4.54	4.72	4.78
CrO(OH)−OH	−0.01	0.14	1.26	3.67	3.90	3.96
CrO_2−OH	0.04	0.10	0.08	4.00	4.24	4.41
CrO_2(OH)−OH	−0.09	0.05	−0.03	3.31	3.37	3.50

[a] Computed according to 1PT/RHF. [b] Zero-point vibrational energy. [c] Basis-set correction computed as outlined in Computational Details. [d] RHF (UHF) for open (closed) shell molecules. [e] Includes an additive correction amounting to 0.105 eV for D_0(CrX−OH). [f] PCI-X extrapolated estimate, with $X = 93.6$ and basis set correction according to ref 30.

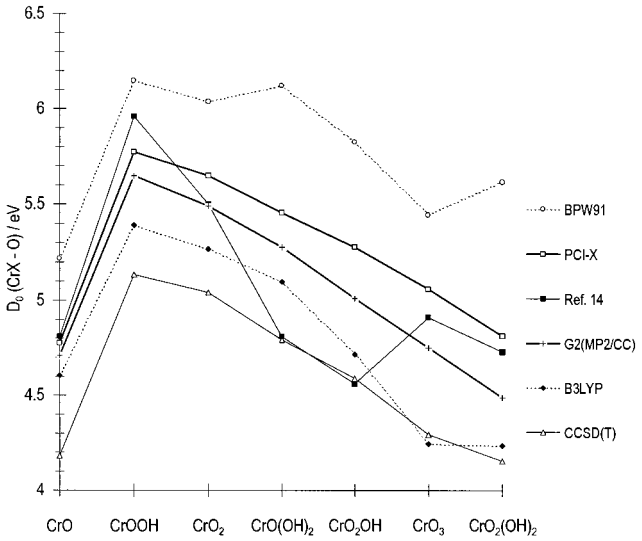

Figure 4. Chromium−oxo bond dissociation energies as computed by various methods. The average of PCI-X and G2(MP2/CC) represents our best estimates.

BPW91 too high by half an electronvolt. A recent DFT study of CrO_2 reports the same binding energy relative to Cr + O_2, as obtained here with the BPW91 functional.[55] The CCSD(T) bond energies are consistently too low by a similar amount, thereby agreeing fairly well with energies obtained by the DFT-HF hybrid method, B3LYP. Even though the trends are reproduced by all methods considered here, the spread is large in absolute terms, and only PCI-X and G2(MP2/CC) energies aspire to quantitative accuracy. Even among bond dissociation energies (BDE's) obtained by these two closely related methods, disagreement grows with increasing oxidation state for chromium to a maximum of 0.32 eV for chromic acid. The reason is that correlation effects are steadily increasing, thereby leading to larger semiempirical correction terms in the PCI-X approach. In fact, with close to 8 eV in the computed contribution from electron correlation to the Cr−oxo BDE in $CrO_2(OH)_2$, it is likely that the multiplicative correction in PCI-X is overshooting, implying nonnegligible second-order terms in the underlying Taylor expansion. On the other hand, a fixed additive correction term, as included in G2 bond dissociation energies, may be too low for the five- and six-valent chromium molecules. Taken together, BDE's obtained by PCI-X and G2(MP2/CC) may be regarded as reasonable estimates of upper and lower limits, respectively, to D_0(CrX−O). One reservation should be taken, though, concerning the applicability of a single-reference correlation method like CCSD(T). For chromic acid, the T_1 diagnostic[56] approaches 0.06, which is high but not unreasonable in connection with a triples correction as included here. Furthermore, the good agreement between RCCSD(T) and UBD(T), as observed for CrO_3 in Table 2, suggests that Hartree−Fock orbitals are quite reasonable even at an oxidation number of VI for Cr. Hence, the average of PCI-X and G2(MP2/CC) extrapolated bond energies, as listed in Tables 8 and 9, may be regarded as "best estimates."

Next, individual computed BDE's are compared with experimental values where available. Unfortunately, only for the monoxide is the Cr−oxo bond strength well-established, at 4.74 ± 0.10 eV,[8] which is equal to our best estimate as obtained by averaging values obtained by G2(MP2/CC) and PCI-X (see Table 8). For the remaining molecules, the comparison will be to bond energies suggested by Ebbinghaus,[12,14] who reviewed the scattered experimental data existing for these molecules. From Figure 4, it appears that our best estimates of Cr−oxo bond strengths agree well with those suggested by Ebbinghaus for the chromium oxides, as well as for chromic acid. This is reassuring, since this subset is better covered by experiments than the remaining molecules, making the resulting bond energies the more reliable. In particular, it is interesting to observe that the PCI-X and G2 estimates bracket the bond energies of chromic acid and its anhydride (cf. the previous paragraph). On the other hand, large deviations between the present work and ref 14 exist for $CrO(OH)_2$ and CrO_2OH and to lesser extent also for chromous acid, CrOOH. As for the former of these molecules, Ebbinghaus employs Dittmer and Niemann's electronegativity correlation[57] and Krikorian's fluoride-to-hydroxide bond energy correlation[15] to obtain the BDE. Even though these correlations provide useful estimates in the lack of experimental values, one may not expect high accuracy. The value for CrO_2OH is based on an reevaluation of vapor pressure data by Kim and Belton.[58] Ebbinghaus suggests that a major constituent, namely, chromic acid, was overlooked in the original analysis and computes its partial pressure from thermochemical data. The partial pressure of CrO_2OH is then obtained by subtraction and used to computed thermodynamical functions. Although this is an interesting analysis, the procedure is prone to cancellation errors that may render the final BDE estimate less reliable. Also, none of the DFT, ab initio, or B3LYP data suggest that oxo bonds in $CrO(OH)_2$ and CrO_2OH should be significantly weaker than those in chromium trioxide. The CrOOH datum in ref 12 is based on a reanalysis of volatility data by Bulewicz and Padley,[59] and Ebbinghaus suggests that the unidentified chromium specimen discussed in that work was in fact chromous acid, CrOOH. Again, it is likely that the indirect route of establishing the Cr−oxo bond energy may lead to large uncertainties. Hence, the presently computed series of BDE's is regarded as the most accurate and consistent available for these molecules.

Computed chromium−hydroxo bond dissociation energies are presented in Figure 5, with the oxidation number of Cr

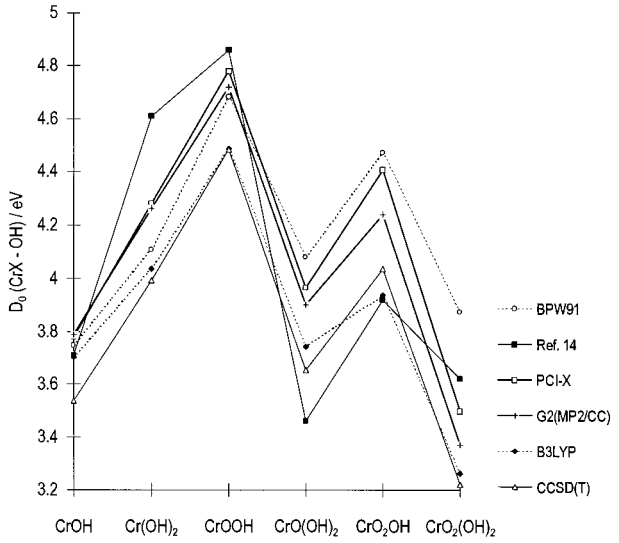

Figure 5. Chromium−hydroxo bond dissociation energies as computed by various methods. The average of PCI-X and G2(MP2/CC) represents our best estimates.

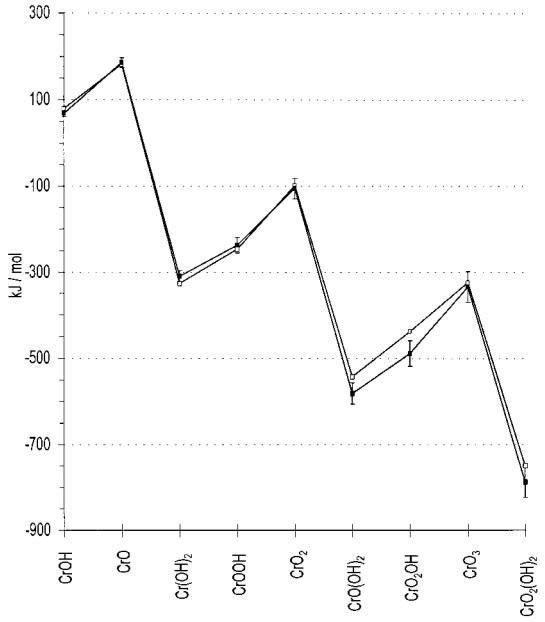

Figure 6. Enthalpies of formation at 298 K, as computed in this work by averaging values obtained by PCI-X and G2(MP2/CC) (■) and estimated by Ebbinghaus[12,14] from experimental data and empirical correlations (□). Error bars included for the computed values are given by 6Ω kJ/mol, where Ω is the formal oxidation number for Cr in each case.

increasing to the right. Again, the highest value is found for CrOOH, where it actually is comparable to the bond strength in chromium monoxide. A second maximum occurs for $CrO_2(OH)$, and for these two molecules, elements of π bonding between chromium and the hydroxo moieties are evident from molecular orbital plots, as discussed for structural implications in a previous section. Apart from this, there is a tendency for lower bond energies at higher oxidation states, as noted for the oxo bonds. The BPW91-based bond energies agree well with our best estimates, apart from the case of chromic acid, $CrO_2(OH)_2$. A similar divergence may be noted for this molecule also with respect to the oxo bond strength (cf. Figure 4), where BPW91 is the only method predicting a Cr−oxo bond in chromic acid that is stronger than that of its anhydride, CrO_3. The agreement between PCI-X and G2(MP2/CC) is highly satisfactory for Cr−OH bond strengths in molecules up to and including $CrO(OH)_2$, with a maximum deviation of 0.06 eV (cf. Table 9). For the dioxohydroxides the deviation doubles, in agreement with observations for the Cr−oxo bond dissociation energy.

The agreement between our best estimates of D_0(CrX−OH) and those presented by Ebbinghaus[14] is excellent for CrOH, fairly good for chromous and chromic acid, and poor for $Cr(OH)_2$, $CrO(OH)_2$, and CrO_2OH. Apart from the pure hydroxides, the discussion presented for Cr−oxo bonds fully addresses these findings. In the case of $Cr(OH)_2$, the enthalpy of formation as quoted in ref 14 is based on Dittmer and Niemann's electronegativity correlation. The resulting BDE may suffer from significant errors, both on account of the inherent inaccuracy in this correlation and through errors with regard to structure and vibrational frequencies. For instance, our optimized bond angle about chromium is 150° for the dihydroxide, in contrast to the linear geometry assumed in ref 12.

3.4.2. Enthalpies of Formation. On the basis of our best estimates of bond dissociation energies and experimental enthalpies of formation for atomic chromium and oxygen as well as gaseous hydroxyl, enthalpies of formation at 298 K are prepared for the nine molecules covered in this study (cf. Table 10). A set of recommended best values are obtained as simple means of the G2(MP2/CC) and PCI-X values. Error bounds for the presented enthalpies of formation are obtained as 6 × Ω kJ/mol, where Ω is the formal oxidation number of chromium in the molecule under consideration, as explained in Computational Details. The enthalpy data are presented in Figure 6, together with corresponding data prepared by Ebbinghaus.[12,14] The agreement between the two series is excellent for the smaller molecules, albeit with a difference of 18 kJ/mol in the case of chromium dihydroxide. However, as discussed above for bond energies, data in ref 14 regarding this molecule are based on

TABLE 10: $\Delta_f H^\circ_{298}$ of Selected Chromium Hydroxides, Oxides, and Oxohydroxides, As Computed in This Work and Compared with Literature Values (All Values in kJ/mol)

molecule	G2(MP2/CC)	PCI-X	recommended[a]	ref 14	NIST database[b]
CrOH	68	67	68	79	
CrO	183	189	186	182	188
$Cr(OH)_2$	−310	−309	−309	−327	
CrOOH	−243	−232	−238	−247	
CrO_2	−117	−96	−106	−99	−75
$CrO(OH)_2$	−590	−571	−580	−542	
CrO_2OH	−507	−469	−488	−438	
CrO_3	−360	−309	−334	−324	−293
$CrO_2(OH)_2$	−812	−762	−787	−748	

[a] Obtained as a simple average of G2(MP2/CC) and PCI-X estimates. [b] H. Y. Afeefy; J. F. Liebman; and S. E. Stein. Neutral Thermochemical Data. In *NIST Chemistry WebBook, NIST Standard Reference Database, Number 69*; Eds. W. G. Mallard, W. G., and P. J. Linstrom, P. J., Eds.; National Institute of Standards and Technology: Gaithersburg MD, March 1998 (http://webbook.nist.gov).

empirical correlations, and deviations of this magnitude are expected. For the dioxide and trioxide of chromium, the presently derived best estimates agree well with enthalpies of formation suggested by Ebbinghaus. On the other hand, standard reference work typically quotes higher energies than obtained here (cf. Table 10), and at least for CrO_2 an update may be appropriate. Turning to the higher, mixed oxohydroxides, sizable deviations are noted between our and Ebbinghaus' data for $CrO(OH)_2$, CrO_2OH, and chromic acid, with the theoretical values systematically at lower enthalpies of formation. For $CrO(OH)_2$ and CrO_2OH, the deviations are clearly significant compared to estimated error bars (cf. Figure 6). The difference is large also for chromic acid, but in this case it is of the same order as the estimated error limit. Furthermore, the spread is also large between G2(MP2/CC) and PCI-X, making it difficult to claim that our computed value is the better. This is certainly a point where further experimental work is welcome.

4. Conclusions

With the notable exception of chromium monoxide, there is an unfortunate lack of thermochemical data for gaseous hydroxides, oxides, and mixed oxohydroxides of chromium. However, Ebbinghaus recently reviewed the situation[14] and prepared a set of tentative enthalpies of formation based on scattered experimental data, molecular structures that to a large extent were anticipated, and various empirical correlations. In the present work, structures, vibrational frequencies, and bond energies have been computed using gradient-corrected DFT and high-level ab initio methods in conjunction with semiempirical extrapolation schemes. This has allowed the preparation of a consistent set of enthalpies of formation of competitive accuracy for a selection of nine molecules obeying the generic formula $CrO_m(OH)_n$. In general, there is good agreement between our computed enthalpies and those suggested in ref 14. However, for three molecules, $Cr(OH)_2$, $CrO(OH)_2$, and CrO_2OH, we suggest adjustments to $\Delta_f H^\circ_{298}$ amounting to +20, −40, and −50 kJ/mol, respectively. For a fourth molecule, chromic acid, our data suggest that the enthalpy of formation listed in ref 14 is too high, even though the uncertainty in our data precludes a stronger conclusion. Hopefully, this study can give the required impetus to further high-quality experimental studies of the thermodynamics of this and related molecules.

Acknowledgment. We thank Dr. Trond Saue who put his Dirac−Hartree-Fock computer code, DIRAC, at our disposal and provided valuable help concerning its use. This work has been supported financially by VISTA and through a grant of computing time from The Research Council of Norway (Programme for Supercomputing).

References and Notes

(1) Minh, N. Q. *J. Am. Ceram. Soc.* **1993**, *76*, 563.
(2) Drenckhahn, W. *Power Eng. J.* **1996**, 67.
(3) Hilpert, K. Interfacial Layers in SOFC−Thermodynamics and Properties. 7th IEA Workshop on Theory and Measurements of Microscale Processes in Solid Oxide Fuel Cells, Wadahl, Norway, 1995.
(4) Hilpert, K.; Das, D.; Miller, M.; Peck, D. H.; Weiss, R. *J. Electrochem. Soc.* **1996**, *143*, 3642.
(5) Linak, W. P.; Ryan, J. V.; Wendt, J. O. L. *Combust. Sci. Technol.* **1996**, *116*, 479.
(6) Kashireninov, O. E.; Fontijn, A. *Combust. Flame* **1998**, *113*, 498.
(7) Kang, H.; Beauchamp, J. L. *J. Am. Chem. Soc.* **1986**, *108*, 5663.
(8) Hedgecock, I. M.; Naulin, C.; Costes, M. *Chem. Phys.* **1996**, *207*, 379.
(9) Espelid, Ø.; Børve, K. J. *J. Phys. Chem. A* **1997**, *101*, 9449.
(10) Grimley, R. T.; Burns, R. P.; Inghram, M. G. *J. Chem. Phys.* **1961**, *34*, 664.
(11) Chase, M. W., Jr.; Curnutt, J. L.; Prophet, H.; McDonald, R. A.; Syverud, A. N. *J. Phys. Chem. Ref. Data* **1975**, *4*, 85−90.
(12) Ebbinghaus, B. B. *Combust. Flame* **1993**, *93*, 119.
(13) Farber, M.; Srivastava, R. D. *Combust. Flame* **1973**, *20*, 43.
(14) Ebbinghaus, B. B. *Combust. Flame* **1995**, *101*, 311.
(15) Krikorian, O. H. *High Temp.−High Pressures* **1982**, *14*, 387.
(16) Glemser, O.; Müller, A. *Z. Anorg. Chem.* **1964**, *334*, 150.
(17) Frisch, M. J.; Trucks, G. W.; Schlegel, H. B.; Gill, P. M. W.; Johnson, B. G.; Robb, M. A.; Cheeseman, J. R.; Keith, T.; Petersson, G. A.; Montgomery, J. A.; Raghavachari, K.; Al-Laham, M. A.; Zakrzewski, V. G.; Ortiz, J. V.; Foresman, J. B.; Peng, C. Y.; Ayala, P. Y.; Chen, W.; Wong, M. W.; Andres, J. L.; Replogle, E. S.; Gomperts, R.; Martin, R. L.; Fox, D. J.; Binkley, J. S.; Defrees, D. J.; Baker, J.; Stewart, J. P.; Head-Gordon, M.; Gonzalez, C.; Pople, J. A. *Gaussian 94*, 2nd ed.; Gaussian, Inc.: Pittsburgh, PA, 1995.
(18) Andersson, K.; Blomberg, M. R. A.; Fülscher, M. P.; Karlström, G.; Lindh, R.; Malmqvist, P.-Å.; Neogrády, P.; Olsen, J.; Roos, B. O.; Sadlej, A. J.; Schütz, M.; Seijo, L.; Serrano-Andrés, L.; Siegbahn, P. E. M.; Widmark, P.-O. *MOLCAS*, 4 ed.; Lund University: Lund, Sweden, 1997.
(19) Becke, A. D. *J. Chem. Phys.* **1993**, *98*, 5648.
(20) Becke, A. D. *Phys. Rev. A* **1988**, *38*, 3098.
(21) Vosko, S. H.; Wilk, L.; Nusair, M. *Can. J. Phys.* **1980**, *58*, 1200.
(22) Lee, C.; Yang, W.; Parr, R. G. *Phys. Rev. B* **1988**, *37*, 785.
(23) Cizek, J. *Adv. Chem. Phys.* **1969**, *14*, 35.
(24) Purvis, G. D., III.; Bartlett, R. J. *J. Chem. Phys.* **1982**, *76*, 1910.
(25) Scuseria, G. E.; Janssen, C. L.; Schaefer, H. F., III. *J. Chem. Phys.* **1988**, *89*, 7382.
(26) Pople, J. A.; Head-Gordon, M.; Raghavachari, K. *J. Chem. Phys.* **1987**, *87*, 5968.
(27) Siegbahn, P. E. M.; Blomberg, M. R. A.; Svensson, M. *Chem. Phys. Lett.* **1994**, *223*, 35.
(28) Siegbahn, P. E. M.; Svensson, M.; Boussard, P. J. E. *J. Chem. Phys.* **1995**, *102*, 5377.
(29) Blomberg, M. R. A.; Siegbahn, P. E. M.; Svensson, M. *J. Chem. Phys.* **1996**, *104*, 9546.
(30) Bauschlicher, C. W., Jr.; Partridge, H. *Chem. Phys. Lett.* **1995**, *245*, 158.
(31) Curtiss, L. A.; Raghavachari, K.; Trucks, G. W.; Pople, J. A. *J. Chem. Phys.* **1991**, *94*, 7221.
(32) Bauschlicher, C. W., Jr.; Partridge, H. *J. Chem. Phys.* **1995**, *103*, 1788.
(33) Wong, M. W. *Chem. Phys. Lett.* **1996**, *256*, 391.
(34) Ziegler, T. *Can. J. Chem.* **1995**, *73*, 743.
(35) Perdew, J. P. *Phys. Rev. B* **1986**, *33*, 8822.
(36) Ziegler, T.; Tschinke, V.; Baerends, E. J.; Snijders, J. G.; Ravenek, W. *J. Phys. Chem.* **1989**, *93*, 3050.
(37) Chong, D. P.; Langhoff, S. R. *J. Chem. Phys.* **1986**, *84*, 5606.
(38) Saue, T. Ph.D. Thesis, University of Oslo, 1995.
(39) Dyall, K. G.; Grant, I. P.; Johnson, C. T.; Parpia, F. A.; Plummer, E. P. *Comput. Phys. Commun.* **1989**, *55*, 425.
(40) Raghavachari, K.; Trucks, G. W.; Pople, J. A.; Head-Gordon, M. *Chem. Phys. Lett.* **1989**, *157*, 479.
(41) Stanton, J. F. *J. Chem. Phys.* **1994**, *101*, 371.
(42) Chen, W.; Schlegel, H. B. *J. Chem. Phys.* **1994**, *101*, 5957.
(43) Lee, T. J.; Kobayashi, R.; Handy, N. C.; Amos, R. D. *J. Chem. Phys.* **1992**, *96*, 8931.
(44) Crawford, T. D.; Stanton, J. F.; Allen, W. D.; Schaefer, H. F., III. *J. Chem. Phys.* **1997**, *107*, 10626.
(45) Bauschlicher, C. W., Jr.; Maitre, P. *Theor. Chim. Acta* **1995**, *90*, 189.
(46) Bader, R. F. W. *Atoms in Molecules: A Quantum Theory*; Oxford University Press: Oxford, 1990.
(47) Cioslowski, J.; Nanayakkara, A.; Challacombe, M. *Chem. Phys. Lett.* **1993**, *203*, 137.
(48) Chertihin, G. V.; Bare, W. D.; Andrews, L. *J. Chem. Phys.* **1997**, *107*, 2798.
(49) Hocking, W. H.; Merer, A. J.; Milton, D. J.; Jones, W. E.; Krishnamurty, G. *Can. J. Phys.* **1980**, *58*, 516.
(50) French, R. J.; Hedberg, L.; Hedberg, K.; Gard, G. L.; Johnson, B. M. *Inorg. Chem.* **1983**, *22*, 892.
(51) Ziegler, T.; Li, J. *Organometallics* **1995**, *14*, 214.
(52) Wenthold, P. G.; Jonas, K.-L.; Lineberger, W. C. *J. Chem. Phys.* **1997**, *106*, 9961.
(53) Yampol'skii, V. I.; Mal'tsev, A. A. *Russ. J. Inorg. Chem.* **1973**, *18*, 137.
(54) Cieslak-Golonka, M. *Coord. Chem. Rev.* **1991**, *109*, 223.
(55) Martínez, A. *J. Phys. Chem.* **1998**, *102*, 1381.
(56) Lee, T. J.; Taylor, P. R. *Int. J. Quantum Chem. Symp.* **1989**, *23*, 199.
(57) Dittmer, G.; Niemann, U. *Mater. Res. Bull.* **1983**, *18*, 355.
(58) Kim, Y.-W.; Belton, G. R. *Metall. Trans.* **1974**, *5*, 1811.
(59) Bulewicz, E. M.; Padley, P. J. *Proc. R. Soc. London, Ser. A* **1971**, *323*, 377.